Astron. Astrophys. 335, L25–L29 (1998)

ASTRONOMY AND ASTROPHYSICS

LETTER

Letter to the Editor

The nucleus and inner coma of Comet 46P/Wirtanen*

P.L. Lamy[1], I. Toth[1,2], L. Jorda[3], H.A. Weaver[4], and M. A'Hearn[5]

[1] Laboratoire d'Astronomie Spatiale, B.P. 8, F-13376 Marseille Cedex 12, France (e-mail: lamy@astrsp-mrs.fr)
[2] Konkoly Observatory, P.O. Box 67, H-1525 Budapest, Hungary
[3] Max-Planck Institut für Aeronomie D-37191 Katlenburg-Lindau, Germany
[4] Department of Physics and Astronomy, Johns Hopkins University, Baltimore, MD 21218, USA
[5] Department of stronomy, University of Maryland, College Park, MD 20742-2421, USA

Received 21 October 1997 / Accepted 10 March 1998

Abstract. We report the detection of the nucleus of comet 46P/Wirtanen from analysis of images taken with the Planetary Camera (WFPC2) of the Hubble Space Telescope (HST) on 28 August 1996. The high spatial resolution (a WFPC2 pixel projects to 50 km at the distance of the comet) allowed us to separate the signal of the nucleus from that of the coma and to determine the Landolt V and R magnitudes of the nucleus. Assuming a spherical body with a geometric albedo of 0.04 and a phase coefficient of 0.04 mag/deg, we derived a radius of 0.60±0.02 km. The color of the nucleus is moderately red with a gradient of 10% per 1000 Å at optical wavelengths. From the lightcurve data we derived a rotational period of 6.0±0.3 hr and find that the ratio of the semi-axes of the assumed ellipsoidal body must satisfy $a/b \geq 1.2$. From an analysis of the dust coma, we derived that $Af\rho$ is 23 cm and that the dust production rate is 4 kg sec^{-1}.

Key words: comets: general – comets: individual: 46P/Wirtanen – telescopes: image processing

1. Introduction

Comet 46P/Wirtanen was discovered in 1948 and is a short–period comet in the Jupiter family. Before it began to attract attention following its selection as the target of the international ROSETTA mission, little was known about its nucleus except for its large non–gravitational acceleration (Rickman et al. 1991), which suggested that a large fraction of its surface is active (Jorda and Rickman 1995).

In 1995, 46P/Wirtanen was marginally detected as a stellar object at a heliocentric distance of 4.6 AU (Boehnhardt et al. 1996). Although this detection has been questioned, the derived faint R-band magnitude of 24.2 implied that the radius of the nucleus was ≤ 0.8 km (assuming an albedo of 0.04), which was already smaller than the value used during preliminary planning of the ROSETTA mission.

Following the successful detection of several cometary nuclei on high resolution images obtained with the Hubble Space Telescope (Lamy and Toth 1995; Lamy et al. 1995, 1996a,b 1997) including that of comet 46P/Wirtanen (Lamy 1996), we present below a detailed characterization of its nucleus as well as its inner coma.

2. Observations

The observations were performed on a single day, 28 August 1996, 200 days before the comet's perihelion passage on 14 March 1997, when it had a heliocentric distance of 2.45 AU and a geocentric distance of 1.51 AU. A sequence of images taken with two broad–band filters was repeated eight times over a 13 hours interval. Three images were taken each orbit: two 600 sec images using the F675W "R" filter ($\bar{\lambda} = 670$ nm, $\Delta\lambda = 89$ nm) followed by a single 500 sec image using the F555W "V" filter ($\bar{\lambda} = 540$ nm, $\Delta\lambda = 123$ nm). This sequence entirely filled the time available during one HST orbit. The quality of the ephemerides was such that the pointing and tracking were excellent, the comet always falling close to the center of the WFPC2 chip. The pixel of 0.0455 arcsec projects to 50 km at the comet and the coma is detected up to approximately 1000 km from the nucleus. All images were processed using the Routine Science Data Processing System at the Space Telescope Science Institute.

3. Data analysis

The key aspect of the data analysis, as already emphasized in our previous articles, is to separate correctly the signal of the nucleus from that of the coma. As a first step, we decided to co-add all the images taken with a given filter during the eight visits and then fit the resulting average images (one each for the

---

Send offprint requests to: P.L. Lamy

* Based on observations made with the NASA/ESA Hubble Space Telescope, obtained at Space Telescope Science Institute, which is operated by the Association of Universities for Research in Astronomy under NASA contract NAS 5-26555

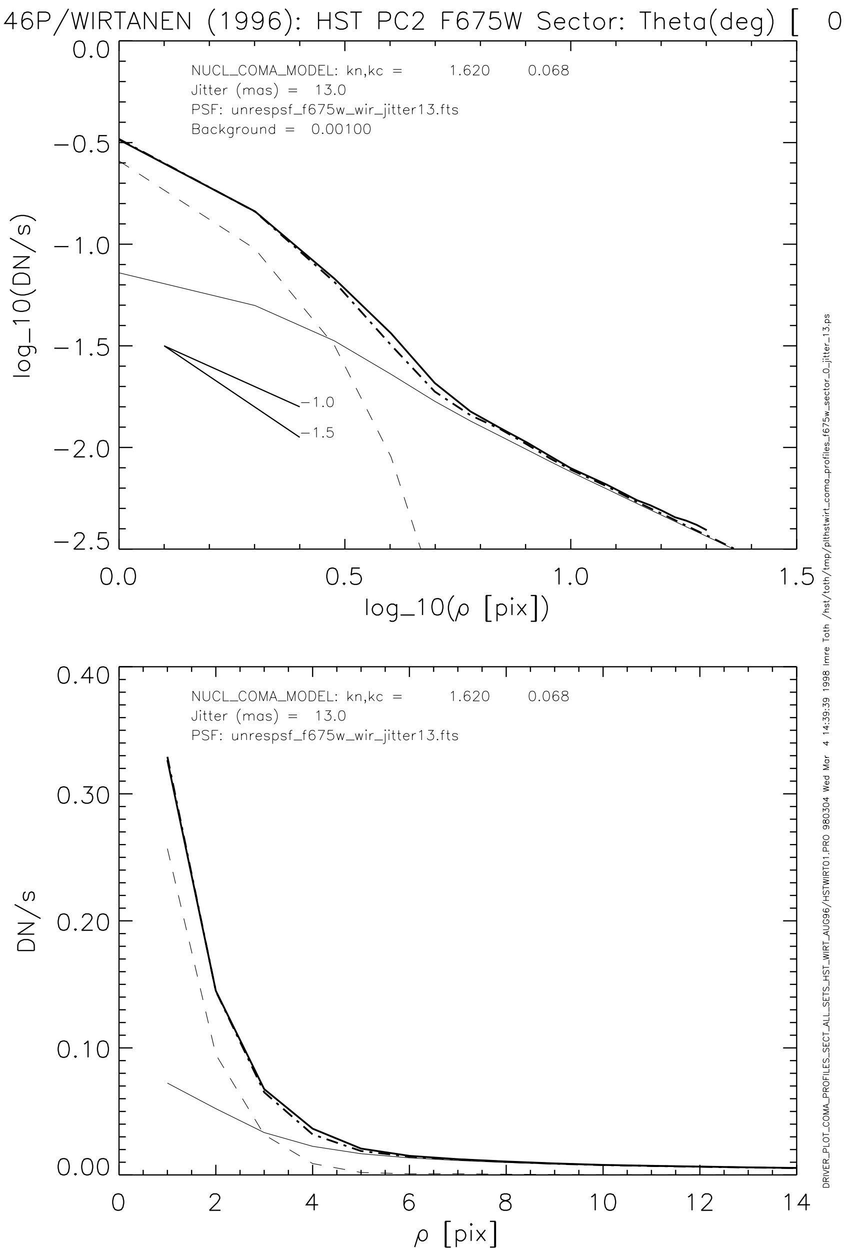

Fig. 1. Azimuthally averaged radial surface brightness profile of the summed F675W image in log-log (top) and linear-linear (bottom) representations. The thick solid line represents the observation, the dashed line is the estimated signal from the nucleus, the thin solid line is the estimated coma, and the dash-dot line is the fitted model.

F675W and F555W cases) to our standard model (Lamy et al. 1995):

$$B(\rho) = \left[k_c/\rho + k_n\delta(\rho)\right] \otimes PSF \qquad (1)$$

In the above equation $\delta(\rho)$ is the Dirac delta function and $\otimes$ is the convolution operator. The first term represents the canonical model of a coma with the scaling factor k_c where the surface brightness decreases as $1/\rho$ where ρ is the distance from the nucleus projected onto the sky plane. This $1/\rho$ function was rigorously calculated in the central 3×3 pixels to take into account the finite extent of the pixels (the effect is negligible beyond that distance). The second term represents the nucleus with the scaling factor of k_n. The Point Spread Functions (PSF) of the telescope were modeled using version 4.0 b of the TinyTIM software written by Krist (1995). One important parameter in the case of long exposures as used here is the jitter of the telescope, which is unknown. We therefore considered several values (0, 10, 13 and 20 milliarcseconds) and generated the corresponding PSFs.

The above assumption on the isotropy of the surface brightness of the coma is not strictly valid as a small azimuthal variation is perceptible. We therefore decided to work with azimuthally averaged radial profiles. This is simply implemented by performing a polar transformation of the images centered on the nucleus (the pixel having the largest signal) with an angular resolution of 1° and summing the 360 individual profiles. Fig. 1 illustrates the results for the F675W filter. The use of azimuthal average images leads to very small 1σ error bars (approximately

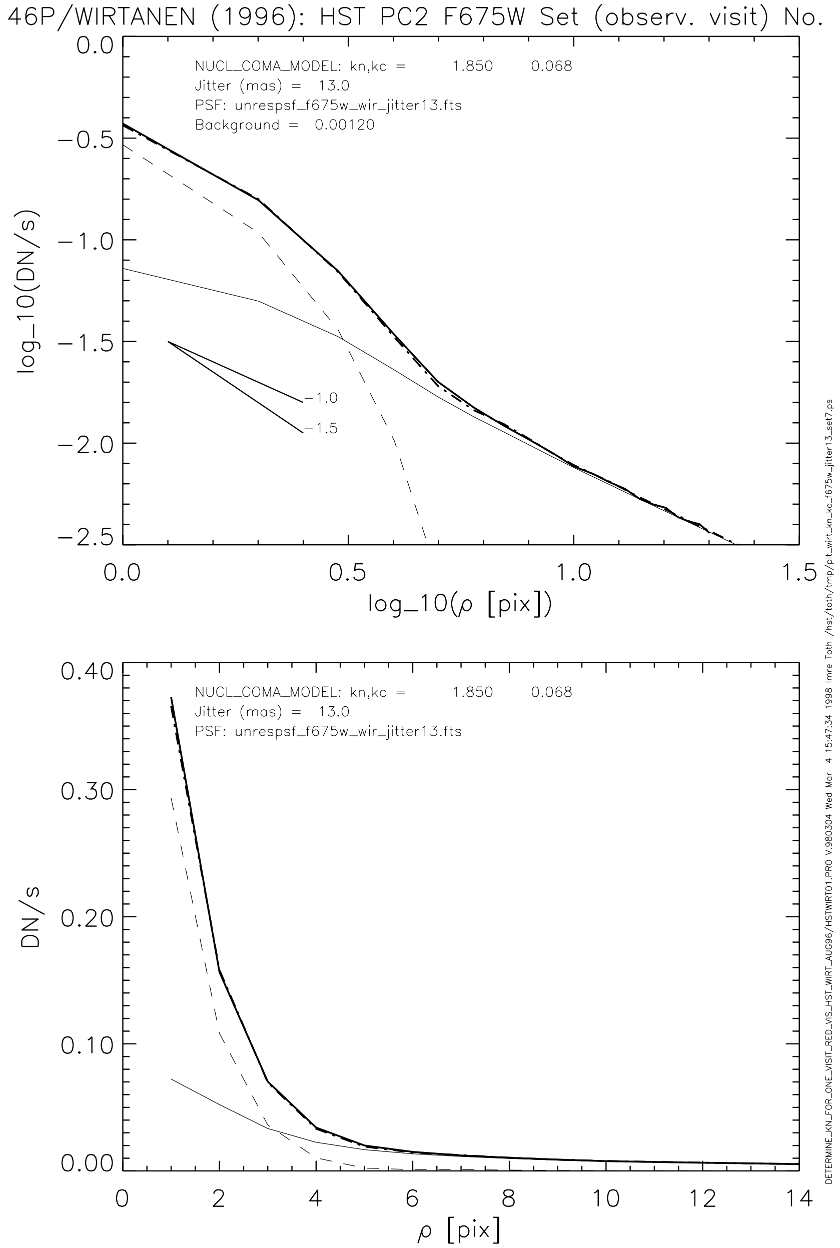

Fig. 2. Azimuthally averaged radial surface brightness profile of the seventh image taken with the F675W filter. See Fig. 1 for explanations.

twice the thickness of the solid line) and were therefore omitted in Fig. 1 for clarity. Several points are worth mentioning.

i) The simple coma model fits the observations extremely well beyond 6 pixels, that is for ρ =300 km. In this region, the gradient in the surface brightness is unaffected by the PSF and is equal to the canonical value -1.

ii) The nucleus is easily detected as its signal exceeds that of the coma in the central pixel by a factor of $\simeq$ 3.5; in other words, the coma signal alone is unable to account for the observations.

iii) The influence of the jitter is perceptible on the core of the image, i.e., up to 3 pixels away from the brightest pixel. Optimal fits have been obtained with jitters of 13 and 10 mas for the F675W and F555W filters, respectively.

In a second step, and in order to look for temporal variations, we individually processed the images from the eight visits. However, we co-added the two consecutive images taken with the F675W filter during each visit to improve the signal-to-noise ratio (S/N). The fit of the standard model (Eq. 1) was thus performed on 16 images. As the averaged radial profiles remain unchanged up to 9 pixels from the central pixel and over the 13 hour interval of the observations, the factors k_c were not allowed to vary but were fixed to the values determined for the summed images (i.e., step 1), after proper scaling according to the exposure times. Fig. 2 illustrates the fit for the seventh image taken with the F675W filter.

The determination of the absolute magnitudes was performed on the $k_n PSF$ images, which measure the brightness of the nucleus as it would be observed by the HST in the absence of coma. The procedure followed the recommendations of Holtzman et al. (1995). The so-called instrumental magnitudes were calculated by integrating the scaled PSFs in an aperture of 0.5 arcsec radius, so that no aperture correction is required. The formulae converting the instrumental WFPC2 magnitudes to the standard Landolt V and R magnitudes require the color corrections (V–R) in first and second orders. However, since we had data in both the V and R filters, we combined the system of two equations in a self-consistent way and could retrieve the V and R magnitudes without making any assumption regarding the color of the nucleus.

4. The properties of the nucleus

Using a standard relationship (Jewitt, 1991), the geometric cross–section of the nucleus and its effective radius can be calculated from its observed magnitude. We assumed a geometric albedo of 0.04 and a linear phase law with a coefficient of 0.04 mag/deg as used in our previous works (Lamy and Toth, 1995; Lamy et al. 1997) We obtained an effective radius of 0.59±0.03 km from the V magnitude and 0.62±0.02 km from the R magnitude. Using an average effective radius of 0.6 km and the canonical value of $\sim$1000 kg m^{-3} for the bulk density, the mass of the nucleus is $\sim$10^{12} kg. We emphasize that the preliminary value of 0.58 km already reported (Lamy 1996) was obtained with a different method in which the fits were performed on horizontal and vertical profiles through the brightest pixel. Our present method, which is far more robust, confirms our initial determination, the agreement resulting from the fact that the nucleus is very easily detected.

Using an albedo of 0.03 increases the radii by 15%, and using an extreme albedo of 0.02 increases it by 41%. Since the observations were obtained at a small phase angle ($\sim$11°), the derived radii are not very sensitive to the particular phase law adopted. A phase law coefficient of 0.03 mag/deg, which closely matches that of the Moon, decreases the radii by 5%. Other sources of uncertainty lead to negligible errors in the derived radii.

The color of the nucleus was calculated from the observed color indices minus the solar color indices and normalized to a value of 1 at 550 nm (the effective wavelength of the V band). The value, calculated from the V and R magnitudes of the nucleus, is $S(\lambda = 640\text{nm}) = 1.09 \pm 0.07$, which is almost identical to the number we derived for the nucleus of comet 45P/Honda–Mrkos–Pajdusakova (Lamy et al. 1997b). The corresponding reflectivity gradient of 10% per 1000 Å is in the middle of the range measured for a variety of comets, even though the sample is small.

The results for the individual V and R apparent magnitudes of the nucleus allowed us to construct a lightcurve for the nucleus (Fig. 3). The lightcurve for the R band clearly suggests that we are seeing the apparent cross–section of a rotating elongated nucleus. The determination of the rotation period P was performed by taking a Fourier decomposition limited to the first sine and cosine terms due to the limited number of data points. The coefficients of these two terms were found using a gradi-

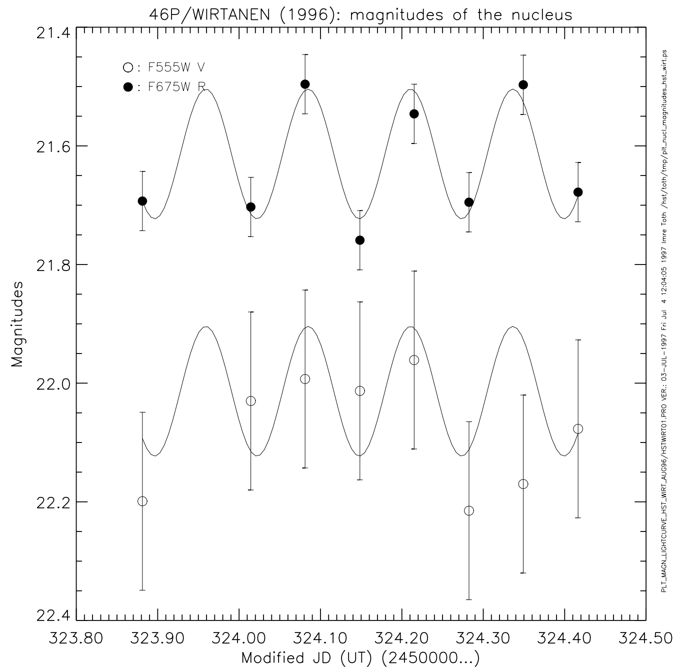

Fig. 3. Temporal variation of the brightness of the nucleus of comet 46P/Wirtanen. The (Landolt) apparent V (circles) and R (dots) observed magnitudes are plotted versus time. The solid lines are the calculated lightcurves.

ent method, and the period was searched in the realistic range of 5 to 20 hr. We found $P = 6 \pm 0.3$ hr, and the corresponding lightcurve is plotted in Fig. 3. Note that this lightcurve is also compatible with the V magnitudes, but not independently confirmed due to the larger uncertainties in this case: the insufficient exposure time of the V images rendered the separation process less accurate compared to the R images. The amplitude of the lightcurve, 0.22 in magnitude, gives only a lower limit on the ratio of the semi–axes, a and b, of an assumed prolate spheroid because the orientation of the spin axis is unknown. We find that $a/b \geq 1.22$. From their ground–based observations of 17 and 18 August 1996, Meech et al. (1997) found a possible rotation period of 7.6 hr and a very small amplitude variation of $\sim$ 0.09 mag. In view of the large amount of coma present in their photometric aperture of 2.5 arcsec radius, the fraction of light contributed by the nucleus is only $\simeq$ 10%. Owing to the far better contrast between the nucleus and the coma during the HST observations, we favor the period derived from the HST data.

5. The properties of the coma

As already pointed out in Sect. 3, no temporal variation of the inner coma could be detected over the 13 hours of the observations. We therefore used the summed images, which offer the highest S/N, to investigate the properties of the coma. The normalized reflectivity of the grains was calculated in a manner similar to that of the nucleus. We derived $S(\lambda = 640\text{nm}) = 1.075 \pm 0.07$, which corresponds to a reflectivity gradient of 8.3% per 1000

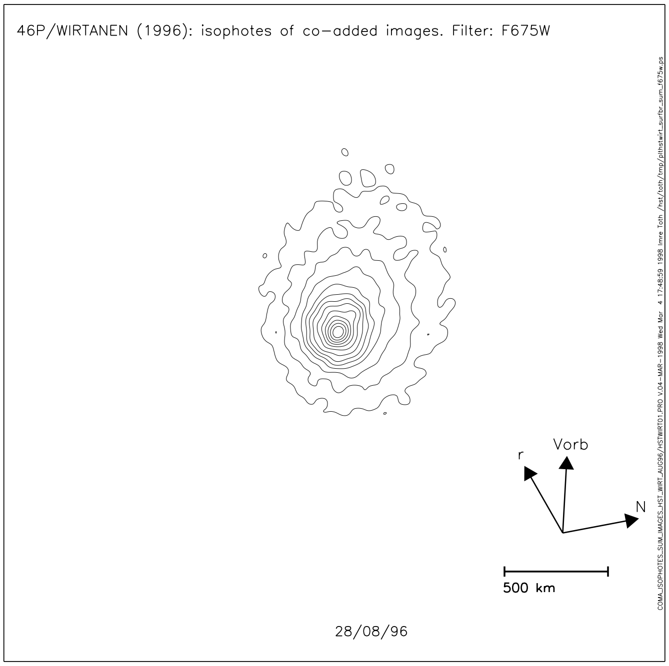

Fig. 4. Isophotal contours of the inner coma for the summed F675W image. The arrows indicate the anti-solar direction (prolonged radius vector r), the direction of celestial North (N), and the heliocentric orbital velocity vector (V_{orb}) of the comet projected onto the sky plane.

Å. This value falls in the range of commonly observed gradients (Meech and Jewitt, 1986), but is probably a lower limit since the F555W filter image may have been contaminated by C_2 emissions.

The azimuthally-averaged coma surface brightness profiles follow a $1/\rho$ law very closely within 800 km of the nucleus (Fig. 1 and 2). However, the coma is not strictly isotropic as the isophotal contours are slightly elongated (Fig. 4, note that the innermost circular contours correspond to the nucleus). Meech et al. (1997) found a coma surface brightness power exponent of -1.62 beyond 1000 km, which likely results from the effect of radiation pressure and an additional mechanism, such as fading grains. We calculated the quantity $Af\rho$ (A'Hearn et al. 1984) from the azimuthally averaged coma profile derived from the summed F675W image (Fig. 1) and obtained a value of 23 cm. This is in excellent agreement with the corrected value obtained by Stern et al. (1998) from their HST observations taken three days earlier with the Faint Object Spectrograph at 295 nm taking into account the reflectivity gradient derived above. Finally, we determined the dust production rate following the method we applied to comet 4P/Faye (Lamy et al. 1996a) and obtained a value of $Q_d = 4.0\,\mathrm{kg\,s^{-1}}$.

6. Conclusions

Our observation confirms the superior capability of the Hubble Space Telescope to detect and characterize cometary nuclei, even when they do not come particularly close to the Earth. Our derived value for the effective radius of the nucleus of comet 46P/Wirtanen of 0.6 km indicates that it belongs to a class of small, highly active nuclei. Since the water production rate at perihelion is 1.7×10^{28} molecules $\mathrm{s^{-1}}$ (cf. Stern et al., 1998), our size for the nucleus implies indeed that as much as 60% of its surface may then be active, using the oversimplified concept and calculation of active area of bare ice at the surface. This large area may not be compatible with the adopted albedo of 0.04, a fact which reinforces the contention of recent models for cometary nuclei that most of the ice is located below the surface. The rotation period of 6 hours makes it one of the fastest rotators among cometary nuclei having well-determined rotational periods. The moderate red color of the nucleus of P/Wirtanen is typical of cometary nuclei. Finally, we derived an $Af\rho$ of 23 cm and a dust production rate of $\sim$4 kg $\mathrm{s^{-1}}$.

Acknowledgements. We express our gratitude to Denise Taylor of the Space Telescope Science Institute for her dedicated efforts in finding suitable guide stars for our observations. This work was supported by a grant from the "Programme National de Planétologie" funded by CNRS and CNES. H.A. Weaver and M.F. A'Hearn acknowledge financial support from NASA through grant number GO-6634 from the Space Telescope Science Institute, which is operated by the Association of Universities for Research in Astronomy, Inc., under NASA contract NAS5-26555.

References

A'Hearn, M.F., D.G. Schleicher, P.D. Feldman, R.L. Millis, and D.T. Thompson, 1984, AJ **89**, 579–591.

A'Hearn, M.F., R.L. Millis, D.G. Schleicher, D.J. Osip, and P.V. Birch, 1995, Icarus **118**, 223–270.

Belyaev, N.A., L. Kresak, E.M. Pittich, and A.N. Pushkarev, 1986, Catalogue of Short-period Comets. Bratislava.

Boehnhardt, H., H. Rauer, S. Mottola, and A. Nathues, 1996. IAU Circ. 6392, May 2, 1996.

Holtzman, J.A., C.J. Burrows, S. Casertano, J.J. Hester, J.T. Trauger, A.M. Watson, and G. Worthey, 1995. PASP **107**, 1065–1093.

Jewitt, D.C., 1991. In Comets in the post-Halley era. R.L. Newburn, M. Neugebauer and J. Rahe, Eds Kluwer Acad. Pub., Dordrecht, Boston, London, pp. 19–65

Jorda, L. and H. Rickman, 1995. PlSpSci **43**, 575–579.

Krist, J., 1995. In *ASP Conference Series Vol.* **77***: Astronomical Data Analysis software and Systems IV*. R.A. Shaw, H.E. Payne, J.J.E. Hayes Eds. pp. 349–352.

Lamy, P.L., 1996, IAUC 6478

Lamy, P.L., and I. Toth, 1995, A&A **293**, L43–L45.

Lamy, P.L., I. Toth, and H.A. Weaver, 1995, BAAS **27**, 1145.

Lamy, P.L., I. Toth, E. Grün, H.U. Keller, Z. Sekanina, and R.M. West, 1996a, Icarus **119**, 370–384.

Lamy, P.L., M.F. A'Hearn, I. Toth, and H.A. Weaver, 1996b, BAAS **28**, 1083.

Lamy, P.L., I. Toth, M.F. A'Hearn, and H.A Weaver, 1997, BAAS **29**, 1029

Meech, K.J., J.M. Bauer, and O.R. Hainaut, 1997, A&A **326**, 1268.

Rickman, H., L. Kamél, C. Froeschlé, and M.C. Festou, 1991. AJ **102**, 1446.

Stern, A.S., J.W. Parker, M.C. Festou, M.F. A'Hearn, P.D. Feldman, G. Schwehm, R. Schulz, J.-L. Bertaux, and D.C. Slater, 1998, A&A this volume